Available online at www.sciencedirect.com
SCIENCE DIRECT®
PERGAMON
International Journal of Engineering Science 41 (2003) 1935–1950
International Journal of Engineering Science
www.elsevier.com/locate/ijengsci

Natural convection on a thin vertical cylinder moving in a high-porosity ambient medium

H.S. Takhar [a,*], A.J. Chamkha [b], G. Nath [c]

[a] *Department of Engineering, Manchester Metropolitan University, John Dalton Building, Chester St., Manchester M1 5GD, UK*
[b] *Department of Mechanical Engineering, Kuwait University, Safat 13060, Kuwait*
[c] *Department of Mathematics, Indian Institute of Science, Bangalore 560016, India*

Received 9 October 2002; accepted 29 January 2003

(Communicated by E.S. ŞUHUBİ)

Abstract

An analysis has been performed to study the natural convection flow over a thin vertical cylinder which is moving with a constant velocity in a non-Darcy high-porosity ambient medium. Both constant wall temperature and constant heat flux conditions have been considered. The coupled non-linear parabolic partial differential equations have been solved numerically by using an implicit finite-difference scheme. The heat transfer is found to be significantly affected by the inertia and porosity parameters, and the Prandtl number, whereas the skin friction is weakly affected. The heat transfer for the constant heat flux case is more than that of the constant wall temperature case and this difference increases with the Prandtl number. The heat transfer increases with the buoyancy force, but the skin friction is slightly reduced.

1. Introduction

The natural convection flow on a vertical surface embedded in porous media occurs in many important engineering problems such as in the design of pebble-bed nuclear reactors, catalytic reactors and compact heat exchangers, in geothermal energy convection, in petroleum reservoirs, in use of fibrous materials in the thermal insulation of buildings, in nuclear wastes etc.

Excellent reviews of the natural convection flows in porous media have been presented by Combarnous and Bories [1], Bejan [2,3] and Tien and Vafai [4]. The non-Darcy effects on the

* Corresponding author. Tel.: +44-161-247-3668.
E-mail address: h.s.takhar@mmu.ac.uk (H.S. Takhar).

0020-7225/03/$ - see front matter
doi:10.1016/S0020-7225(03)00109-5

natural convection boundary layer on an isothermal vertical flat plate immersed in a high-porosity medium were studied by Chen et al. [5]. Chen and Lin [6] extended the analysis of Chen et al. [5] to include the effect of thermal stratification. Chamkha [7] further extended the analysis of Chen and Lin to include the effects of the magnetic field. Minto et al. [8] have studied the natural convection flow driven by an exothermic reaction on a vertical surface embedded in porous media. The natural convection flow being driven by an exothermic reaction over a vertical surface embedded in porous media. Rees and Pop [9] examined the effect of the variable permeability on the free convection flow on a vertical surface in a porous medium.

Flow over cylinders is considered to be two-dimensional if the body radius is large compared to the boundary layer thickness. For a thin or slender cylinder, the radius of the cylinder may be of the same order as the boundary layer thickness. Therefore, the flow may be considered as axisymmetric instead of two-dimensional. In this case, the governing equations contain the transverse curvature term which influences both the velocity and temperature fields. The effect of the transverse curvature is important in certain applications such as wire and fibre drawing where an accurate prediction is required and a thick boundary layer can exist on slender or near slender bodies. The natural convection from the outer surface of an isothermal vertical thin cylinder was investigated by a number of authors [10–17]. The methods that were used to solve this problem are, the heat balance integral [10,11], local non-similarity [12], two-point finite-difference [13], the perturbation expansion [14–16] and the method of extended perturbation series [17]. Recently, Pantokratoras [18] considered the natural convection flow of pure and saline water over a vertical iso-thermal cylinder and obtained the solution by using an implicit finite-difference scheme.

The flow and heat transfer in the boundary layer induced by a surface moving with uniform velocity in an otherwise ambient fluid have many applications in the field of metallurgy and chemical engineering. Sakiadis [19] was the first to study the boundary layer velocity in an ambient fluid. However, his investigation was restricted to the momentum transfer in the boundary layer. Bourne and Elliston [20] extended the above problem by including the energy equation. In [19,20], Karman–Pohlhausen integral technique was used. The accuracy of the integral solutions was tested by Karnis and Pechoc [21] who used a power-series expansion procedure. According to their study, the Karman–Pohlhausen method under estimates the Nusselt number by 8–10% in the range $0.7 \leqslant Pr \leqslant 10$. Choi [22] examined the effect of variable properties of air on the boundary layer flow over a cylinder moving with a constant velocity in an ambient fluid and obtained the solution by using a finite-difference scheme. Na and Pop [23] studied the flow and heat transfer problem over a longitudinal circular cylinder moving in a parallel or reversely to a free stream and obtained the solution of the governing equations by using a finite-difference method. The above studies [19–23] dealt with the forced convection flow and the effect of the buoyancy forces was not considered.

This analysis considers the natural convection flow over a thin vertical cylinder moving with a constant velocity in a non-Darcy high-porosity ambient medium. Both constant wall temperature and constant heat flux conditions are included in the analysis. The coupled non-linear parabolic partial differential equations governing the flow have been solved numerically by using an implicit finite-difference scheme similar to that of Blottner [24]. The results have been compared with those of Karnis and Pechc [21], Tsou et al. [25], Erickson et al. [26], Griffin and Thorne [27] and Moutsoglou and Chen [28].

2. Analysis

Let us consider a thin vertical circular cylinder of radius R maintained at a uniform temperature T_w or at a uniform heat flux q_w and convecting naturally to an environment at temperature T_∞. The radial coordinate r is measured from the axis of the cylinder and the axial coordinate x is measured vertically upward such that $x = 0$ corresponds to the leading edge where the boundary layer thickness is zero. The cylinder moves with a constant velocity U_0 along the axial direction x in a non-Darcy high-porosity medium. Fig. 1 shows the physical model and the coordinate system. The fluid properties are assumed to be constant except the density changes which give rise to the buoyancy forces. Under the above assumptions, the equations of continuity, momentum and energy under boundary layer approximations governing the natural convection flow over a thin vertical cylinder in a non-Darcy high-porosity medium can be expressed as [6,7,12,21,23]:

$$\frac{\partial}{\partial x}(ru) + \frac{\partial}{\partial r}(rv) = 0, \tag{1}$$

$$\varepsilon^{-2}\left(u\frac{\partial u}{\partial x} + v\frac{\partial u}{\partial r}\right) = g\beta(T - T_\infty) + \varepsilon^{-1}\frac{\nu}{r}\frac{\partial}{\partial r}\left(r\frac{\partial u}{\partial r}\right) - \frac{\nu}{K^*}u - C^*u^2, \tag{2}$$

$$u\frac{\partial T}{\partial x} + v\frac{\partial T}{\partial r} = \frac{\alpha}{r}\frac{\partial}{\partial r}\left(r\frac{\partial T}{\partial r}\right). \tag{3}$$

The boundary conditions are the no-slip conditions at the surface and the ambient conditions far away from the surface and these are expressed as,

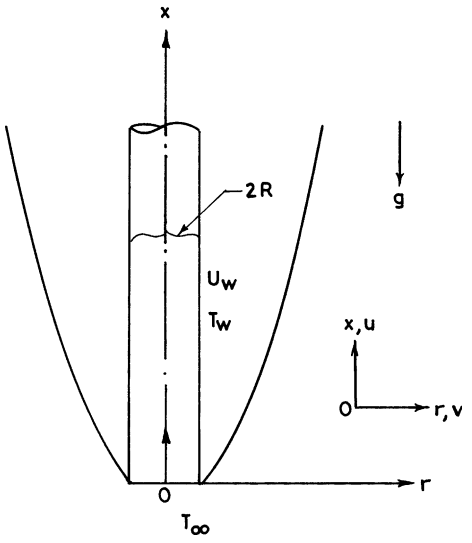

Fig. 1. Physical model and coordinate system.

$$
\begin{aligned}
&u(x,R)=U_0, \quad v(x,R)=0, \quad u(x,\infty)=0, \quad T(x,\infty)=T_\infty,\\
&T(x,R)=T_w \text{ for the constant wall temperature case (CWT case)},\\
&\partial T(x,R)/\partial r=-q_w/K_1 \text{ for the constant heat flux case (CSH case)},\\
&u(o,r)=0, \quad T(0,r)=T_\infty, \quad r>R.
\end{aligned} \tag{4}
$$

Here x and r are the axial and radial coordinates, respectively; u and v are the velocity components along the x and r directions respectively; T is the temperature; v is the kinematic viscosity; ε is the porosity; K^* is the permeability of the medium; C^* is the inertia coefficient; g is the acceleration due to the gravity; β is the volumetric coefficient of thermal expansion; α is the thermal diffusivity; R is the radius of the cylinder; U_0 is the uniform velocity of the cylinder; q_w is the surface heat flux, K_1 is the thermal conductivity; and the subscripts w and ∞ denote conditions at the wall and in the ambient fluid, respectively.

It is convenient to reduce the number of equations from three to two as well as to transform them to dimensionless form. This can be done by applying the following transformations

$$
\begin{aligned}
&\xi=2R^{-1}(vx/U_0)^{1/2}, \quad \eta=(2R)^{-1}(r^2-R^2)(U_0/vx)^{1/2},\\
&u=r^{-1}\partial\psi/\partial r, \quad v=-r^{-1}\partial\psi/\partial x,\\
&\psi(x,r)=R(vU_0x)^{1/2}f(\xi,\eta), \quad T-T_\infty=(T_w-T_\infty)\theta(\xi,\eta),\\
&Gr=g\beta(T_w-T_\infty)R^3/v^2, \quad Re=U_0R/v, \quad \lambda=Gr/Re, \quad K=K^*/R^2,\\
&C=RRe\ C^*, \quad Pr=v/\alpha, \quad u=U_0f'(\xi,\eta),\\
&v=-(R/r)(vU_0/x)^{1/2}[2^{-1}f+\xi\partial f/\partial\xi-\eta f']
\end{aligned} \tag{5}
$$

to Eqs. (1)–(3) and we find that (1) is identically satisfied and (2) and (3) for the constant wall temperature case (CWT case) reduce to,

$$
\begin{aligned}
&\varepsilon^{-1}(1+\xi\eta)f'''+(2\varepsilon)^{-1}(\xi+\varepsilon^{-1}f)f''+(\xi/2)^2(\lambda\theta-K^{-1}f'-Cf'^2)\\
&\quad=\varepsilon^{-2}\xi(f'\partial f'/\partial\xi-f''\partial f/\partial\xi),
\end{aligned} \tag{6}
$$

$$
Pr^{-1}(1+\xi\eta)\theta''+2^{-1}(Pr^{-1}\xi+f)\theta'=\xi(f'\partial\theta/\partial\xi-\theta'\partial f/\partial\xi). \tag{7}
$$

The boundary conditions (4) for the CWT case can be expressed as

$$
f(\xi,0)=0, \quad f'(\xi,0)=1, \quad \theta(\xi,0)=1, \quad f'(\xi,\infty)=\theta(\xi,\infty)=0. \tag{8}
$$

Similarly, the governing equations for the constant heat flux case (CHF case) can be written as

$$
\begin{aligned}
&\varepsilon^{-1}(1+\xi\eta)f'''+(2\varepsilon)^{-1}(\xi+\varepsilon^{-1}f)f''+(\xi/2)^3\lambda^*\theta-(\xi/2)^2(K^{-1}f'+Cf'^2)\\
&\quad=\varepsilon^{-2}\xi(f'\partial f'/\partial\xi-f''\partial f/\partial\xi),
\end{aligned} \tag{9}
$$

$$Pr^{-1}(1+\xi\eta)\theta'' + 2^{-1}(Pr^{-1}\xi + f)\theta' - 2^{-1}f'\theta = \xi(f'\partial\theta/\partial\xi - \theta'\partial f/\partial\xi) \tag{10}$$

with the boundary conditions

$$f(\xi,0) = 0, \quad f'(\xi,0) = 1, \quad \theta'(\xi,0) = -1, \quad f'(\xi,\infty) = \theta(\xi,\infty) = 0, \tag{11}$$

where

$$T(x,r) - T_\infty = (q_w/K_1)(vx/U_0)^{1/2}\theta(\xi,\eta), \quad \lambda^* = Gr^*/Re, \quad Gr^* = g\beta q_w R^4/(K_1 v^2). \tag{12}$$

Here ξ and η are the transformed coordinates; ψ and f are the dimensional and dimensionless stream functions, respectively; f' is the dimensionless velocity in the axial direction; θ is the dimensionless temperature; Pr is the Prandtl number; Re is the Reynolds number; Gr and Gr^* are the Grashof numbers for the CWT and CHF cases, respectively; λ and λ^* are the buoyancy parameters for the CWT and CHF cases, respectively; K is the dimensionless permeability parameter; C is the dimensionless interia coefficient; and a prime denotes derivative with respect to η.

It may be remarked that equations governing the flow over the vertical cylinder can be reduced to those of the flat plate if $R \to \infty$ ($\xi\eta \to 0$). Eqs. (6) and (7) for $\lambda = 0$ (without buoyancy force), $\varepsilon = 1$ (uniform medium), $K^{-1} = C = 0$ (in the absence of the permeability and inertia parameters), $R \to \infty$ (flat plate case), $\xi = 0$ (self-similar flow) area identical to those of [25–27]. Further, for $\varepsilon = 1$, $K^{-1} + C = 0$, $R \to \infty$ ($\xi\eta = 0$), Eqs. (6) and (7) are the same as those of Moutsoglou and Chen [28] if we replace $\lambda\xi$ by ξ_1. Here $\xi\partial/\partial\xi = \xi_1\partial/\partial\xi_1$. Also for $\lambda = K^{-1} = C = 0$, $\varepsilon = 1$, Eqs. (6) and (7) reduce to those of Karnis and Pechoo [21].

The quantities of physical interest are the local Nusselt number Nu_x and the local skin friction coefficient Cf_x and these are expressed as

$$\begin{aligned} Nu_x &= -x(\partial T/\partial r)_{r=2}/(T_w - T_\infty) = -Re_x^{1/2}\theta'(\xi,0) \text{ for CWT case,} \\ Nu_x &= Re_x^{1/2}/\theta(\xi,0) \text{ for the CHF case,} \\ C_{fx} &= -\mu(\partial u/\partial r)_{r=R}/\rho U_0^2 = -Re_x^{-1/2}f''(\xi,0), \end{aligned} \tag{13}$$

where μ is the coefficient of viscosity and ρ is the density of the fluid.

3. Method of solution

Eqs. (6) and (7) under conditions (8) and Eqs. (9) and (10) under conditions (11) have been solved by using an implicit, iterative tridiagonal finite-difference scheme similar to that of Blottner [24]. All the first-order derivatives with respect to ξ have been replaced by two-point backward difference formulae

$$\partial M/\partial\xi = (M_{i,j} - M_{i-1,j})/\Delta\xi \tag{14}$$

where M represents any dependent variable f or θ, and i and j are the node locations along the ξ and η directions. Equations (6) and (9) are converted into second-order equations by substituting

$f' = F$. Then the second-order partial differential equations are discretized by using three-point central difference formulae and all the first-order derivatives with respect to η are discretized by employing the trapezoidal rule. The non-linear terms are evaluated at the previous iteration. At each step of constant ξ, a system of algebraic equations have been solved iteratively by using the Thomas algorithm [24]. The same procedure is repeated for the next ξ value and the equations are solved line by line until the desired ξ value is reached. A convergence criterion based on the relative difference between the current and previous iterations is used. When this difference reaches 10^{-5}, the solution is assumed to have converged and the iterative process is terminated.

We have carried out the sensitivity analysis of the effect of step sizes $\Delta\eta$ and $\Delta\xi$, and the edge of the boundary layer η_∞ on the solution. Finally, the computations were carried out with $\Delta\eta = 0.05$, $\Delta\xi = 0.025$, $\eta_\infty = 25$.

4. Results and discussion

Eqs. (6) and (7) under conditions (8) and Eqs. (9) and (10) under conditions (11) have been solved numerically by using an implicit finite-difference scheme as described earlier. In order to validate our results, we have compared the velocity profile $u/U_0 = f'$ for $\lambda = K^{-1} = C = 0$ (without buoyancy force, inertia and permeability parameters), $\varepsilon = 1$ (uniform medium), $\xi = 0$ (self-similar flow) with the theoretical and experimental results of Tsou et al. [25]. The comparison is shown in Fig. 2. The velocity profile is found to be in very good agreement with the theoretical results. It also agrees well with the experimental results near the wall. Further, the Nusselt number Nu_x for the CWT case when $\lambda = K^{-1} = C = 0$, $\varepsilon = 1$ has been compared with the theoretical values of Erickson et al. [26] and the experimental values of Griffin and Thorne [27]. The comparison is presented in Fig. 3. The results are found to be in good agreement with the theoretical and experimental values when the wall velocity $U_0 \geqslant 8.92$. We have also compared the Nusselt number ($Re_x^{-1/2} Nu_x$) for the CWT case when $\lambda = K^{-1} = C = 0$, $\varepsilon = 1$ with that of Karnis and Pechoc [21]. The results are found to be in good agreement and the comparison is presented in

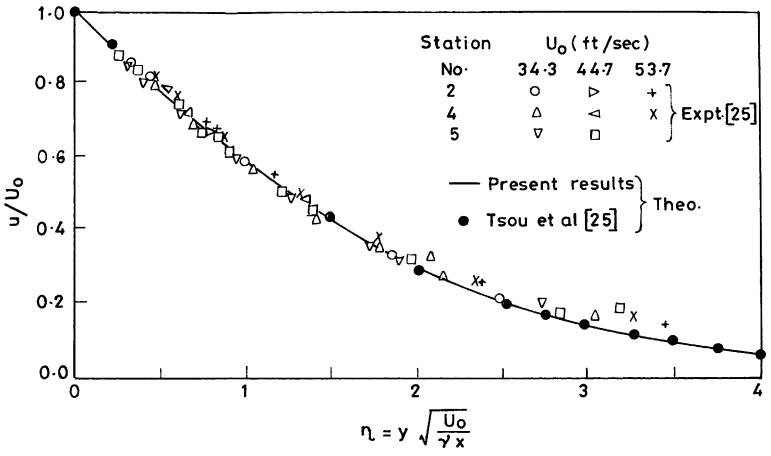

Fig. 2. Comparison of the velocity profile u/U_0 for $\xi = \lambda = K^{-1} = C = 0$, $\varepsilon = 1$ with that of Tsou et al. [25].

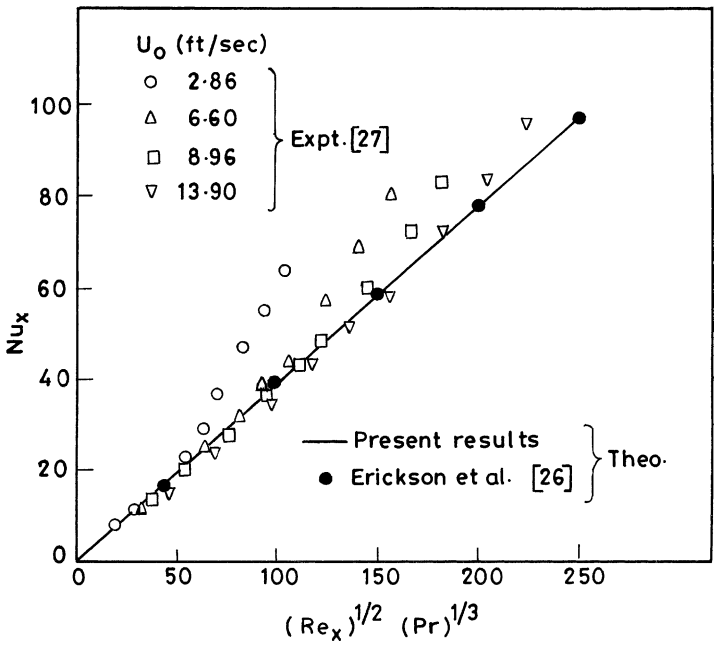

Fig. 3. Comparison of the Nusselt number Nu_x for the CWT case when $\xi = \lambda = K^{-1} = C = 0$, $\varepsilon = 1$ with that of Erickson et al. [26] and Griffin and Thorne [27].

Table 1. The surface shear stress $(-f''(\xi_1, 0))$ and the surface heat transfer $(-\theta'(\xi_1, 0))$ for the CWT case when $\varepsilon = 1$, $K^{-1} = C = 0$, $R \to \infty$ $(\xi\eta = 0)$ have been compared with those of Moutsoglou and Chen [28]. For direct comparison we have to replace $\lambda\xi$ by ξ_1. Hence $\xi\partial/\partial\xi = \xi_1\partial/\partial\xi_1$. These results are in excellent agreement. The comparison is given in Table 2.

Figs. 4 and 5 present the effect of the buoyancy force λ or λ^* on the skin friction coefficient and the Nusselt number $(Re_x^{1/2}Cf_x, Re_x^{-1/2}Nu_x)$ for both CWT and CHF cases when $C = 100$, $K^{-1} = 1$, $Pr = 5.4$, $\varepsilon = 0.9$. The Nusselt number for the CHF case is found to be significantly higher than that of the CWT case, but its effect on the skin friction coefficient is rather small. The reason for this trend is that for the CHF case the wall temperature for $Pr = 5.4$ is much lower than that of the

Table 1
Comparison of heat transfer results $(Re_x^{-1/2}Nu_x)$ for the constant wall temperature case when $\lambda = K^{-1} = C = 0$, $\varepsilon = 1$

ξ	Present results		Karnis and Pechoc [21]	
M	$Pr = 0.7$	$Pr = 1.0$	$Pr = 0.7$	$Pr = 1.0$
0.0001	0.35144	0.44411	0.35288	0.44754
0.001	0.35434	0.44761	0.36070	0.45570
0.005	0.36261	0.45613	0.37467	0.47026
0.01	0.37054	0.46427	0.38499	0.48103
0.04	0.40504	0.49895	0.41930	0.51682
0.05	0.41443	0.50817	0.42719	0.52506
0.06	0.42328	0.51667	0.43425	0.53243

Table 2
Comparison of surface shear stresses, $f''(\xi_1,0)$ and the surface heat transfer, $-\theta'(\xi_1,0)$ for the constant wall temperature case when $K^{-1}=C=0$, $\varepsilon=1$, $R\to\infty(\xi\eta=0)$

Pr	ξ_1	Present results		Moutsoglou and Chen [28]	
		$f''(\xi_1,0)$	$-\theta'(\xi_1,0)$	$f''(\xi_1,0)$	$-\theta'(\xi_1,0)$
0.7	0	−0.44372	0.34922	−0.44915	0.34924
0.7	0.5	−0.10556	0.41317	−0.10558	0.41320
0.7	1.0	0.119423	0.45502	0.19425	0.45505
0.7	1.5	0.47217	0.47761	0.47214	0.47764
0.7	2.0	0.73556	0.50035	0.73552	0.50031
0.7	3.0	1.23107	0.53685	1.23103	0.53681
0.7	4.0	1.69657	0.56613	1.69652	0.56609
0.7	5.0	2.13993	0.59090	2.13988	0.59086
0.7	0	−0.44372	1.38698	−0.28376	1.41322
0.7	0.5	−0.28373	1.41317	−0.44375	1.38703
0.7	1.0	0.02107	1.43706	−0.12876	1.43712
0.7	1.5	−0.12874	1.45932	0.02105	1.45938
0.7	2.0	0.16883	1.48032	0.16880	1.48026
0.7	3.0	0.45321	1.53647	0.45318	1.53641
0.7	4.0	0.72694	1.55340	0.72697	1.55334
0.7	5.0	0.99207	1.58517	0.99201	1.58510

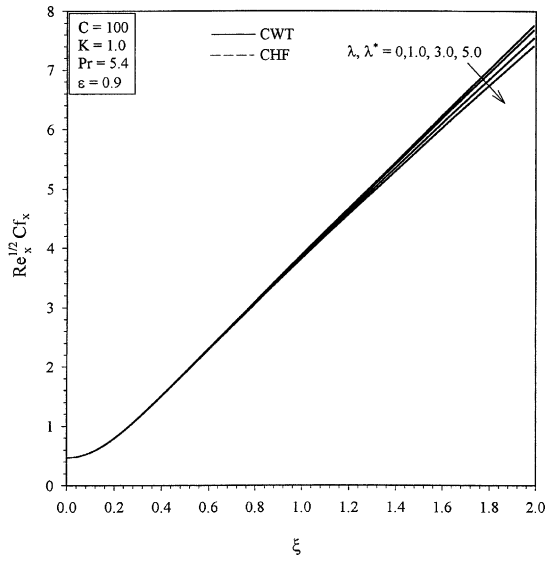

Fig. 4. Effect of λ or λ^* on $Re_x^{1/2}Cf_x$ for CWT and CHF cases.

CWT case. Also the thermal boundary layer thickness for the CHF case is less than that of the CWT case. This results in higher Nusselt number for the CHF case as compared to that of the CWT case. However, the skin friction ($Re_x^{1/2}Cf_x$) is affected very little. Hence the results for the CHF case are rather indistinguishable from those of the CWT case on this scale. The reason for very weak dependence is that the wall conditions have only indirect effect on the momentum

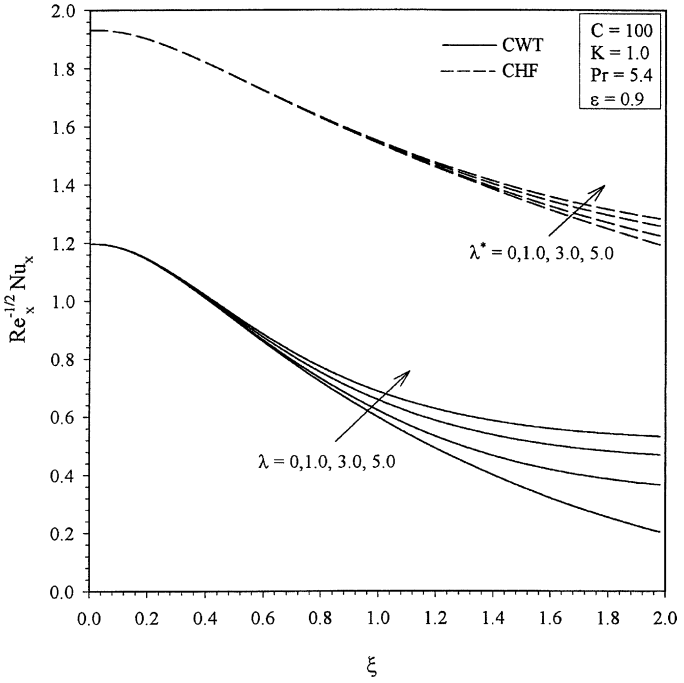

Fig. 5. Effect of λ or λ^* on $Re_x^{-1/2}Nu_x$ for CWT and CHF cases.

equation. Since the positive buoyancy force (λ or $\lambda^* > 0$) implies favourable pressure gradient, the fluid motion within the boundary layer is accelerated causing reduction in the thermal boundary layers. Consequently, the Nusselt number for the CWT and CHF cases increases with λ or λ^*. On the other hand, there is a slight reduction in the skin-friction coefficient ($Re_x^{1/2}Cf_x$) with increasing λ or λ^*. As λ or λ^* increases, fluid velocity near the wall increases, but the difference between the wall and fluid velocities decreases. This results in slight reduction in the skin friction with increasing λ or λ^*. The effect of the buoyancy parameter λ or λ^* increases with the curvature parameter ξ, because λ or λ^* is multiplied by ξ (see Eqs. (6) and (9)). Further, for a fixed λ or λ^* the skin friction increases with ξ, but the Nusselt number decreases. This is due to the fact that the momentum boundary layer reduces with increasing ξ which results in lower value of the radial velocity f. This reduction in f causes a reduction in the Nusselt number. On the other hand, the skin friction increases with ξ due to a reduction in the momentum boundary layer thickness.

Figs. 6 and 7 display the effect of the porosity parameter ε on the velocity and temperature profiles ($f'(\xi,\eta)$, $\theta(\xi,\eta)$ for both CWT and CHF cases for $C = 100$, $K = 1$, $Pr = 5.4$, λ or $\lambda^* = 3$, $\xi = 1$. Since $\varepsilon = 1$ corresponds to a uniform medium, decreasing ε implies less resistance is offered by the medium. Consequently, the axial velocity ($f'(\xi,\eta)$) is increased as ε is reduced, but the temperature $\theta(\xi,\eta)$ is reduced.

The effect of the porosity parameter ε on the skin friction coefficient and the Nusselt number ($Re_x^{1/2}Cf_x$, $Re_x^{-1/2}Nu_x$) for both CWT and CHF cases are shown in Figs. 8 and 9 when $C = 100$, $K = 1$, $Pr = 5.4$, $\lambda = \lambda^* = 3$. The skin friction coefficient increases with ε, but the Nusselt number decreases. This is due to the fact that the velocity gradient increases with ε, but the temperature

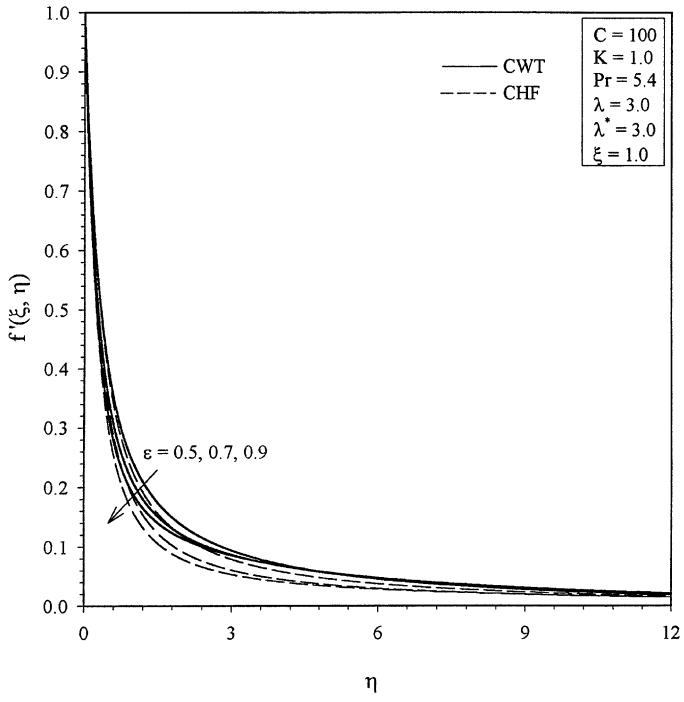

Fig. 6. Effect of ε on $f'(\xi,\eta)$ for CWT and CHF cases.

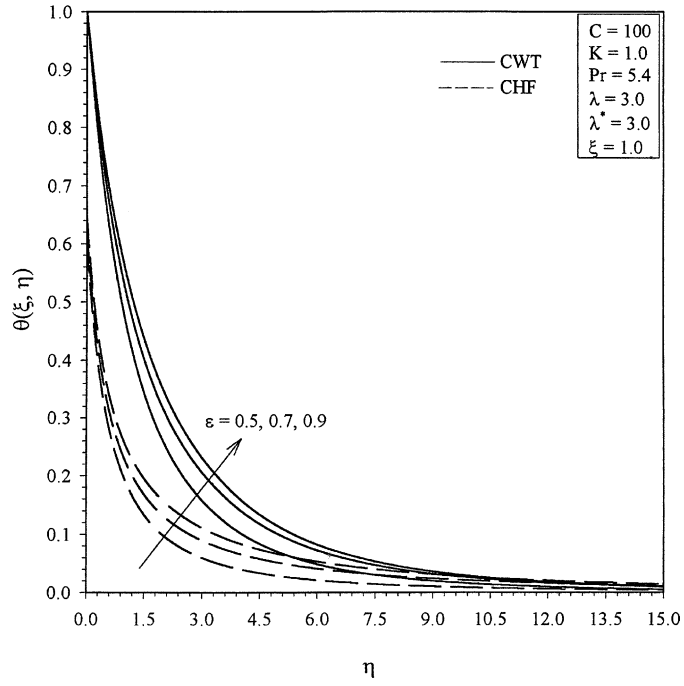

Fig. 7. Effect of ε on $\theta(\xi,\eta)$ for CWT and CHF cases.

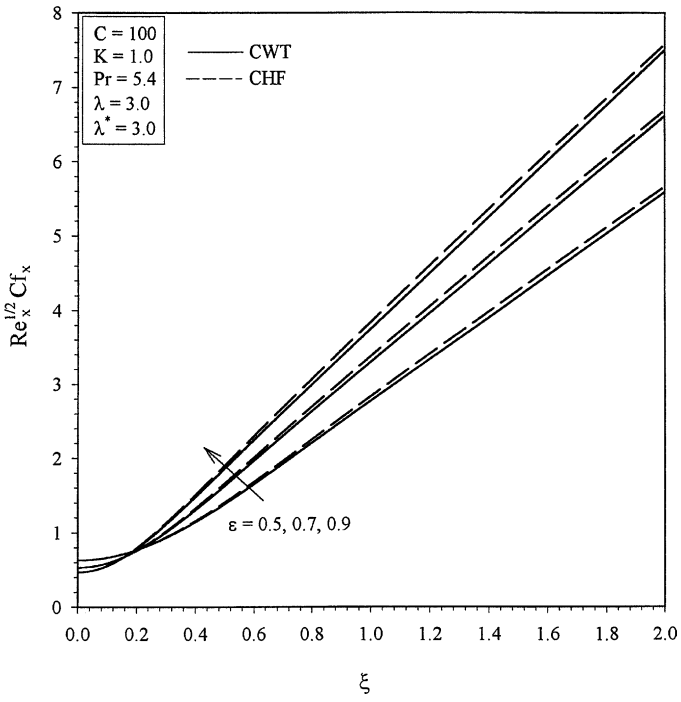

Fig. 8. Effect of ε on $Re_x^{1/2}Cf_x$ for CWT and CHF cases.

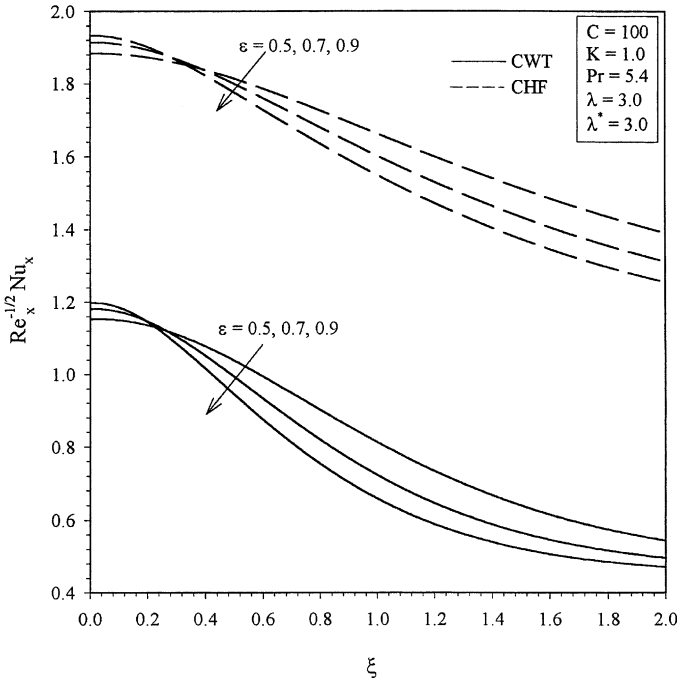

Fig. 9. Effect of ε on $Re_x^{-1/2}Nu_x$ for CWT and CHF cases.

gradient decreases. In the range of $0 \leqslant \xi < 0.3$, an opposite trend is observed. As mentioned earlier, the constant wall temperature and constant heat flux boundary conditions have stronger effect on the Nusselt number than on the skin friction.

Figs. 10 and 11 present the effect of the permeability parameter K on the skin friction coefficient and the Nusselt number ($Re_x^{1/2}Cf_x$, $Re_x^{-1/2}Nu_x$) for both CWT and CHF cases when $C = 100$, $Pr = 5.4$, $\varepsilon = 0.9$, $\lambda = \lambda^* = 3$. It can be seen that both skin friction and Nusselt number are weakly dependent on K.

Figs. 12 and 13 display the effect of the inertia parameter C on the skin friction coefficient and the Nusselt number ($Re_x^{1/2}Cf_x$, $Re_x^{-1/2}Nu_x$) for both CWT and CHF cases when $K = 1$, $Pr = 5.4$, $\varepsilon = 0.9$, $\lambda = \lambda^* = 3$. The inertia parameter C is found to have significant effect on both skin friction and Nusselt number. As C increases, the fluid motion in the boundary layer is accelerated causing reduction in the momentum boundary layer. Consequently, the velocity gradient and hence the skin friction coefficient increase with C. On the other hand, the radial velocity $f(\xi, \eta)$ decreases with increasing C due to the reduction in the boundary layer thickness. Consequently, the Nusselt number decreases with increasing C.

Fig. 14 shows the effect of the Prandtl number Pr on the Nusselt number ($Re_x^{-1/2}Nu_x$) for both CWT and CHF cases when $C = 100$, $K = 1$, $\varepsilon = 0.9$, $\lambda = \lambda^* = 3$. The increase in the Prandtl number implies thinning of thermal boundary layer. Hence the temperature gradient and Nusselt number increases with Pr. This trend is valid for both CWT and CHF cases as well as for all values of the curvature parameter ξ.

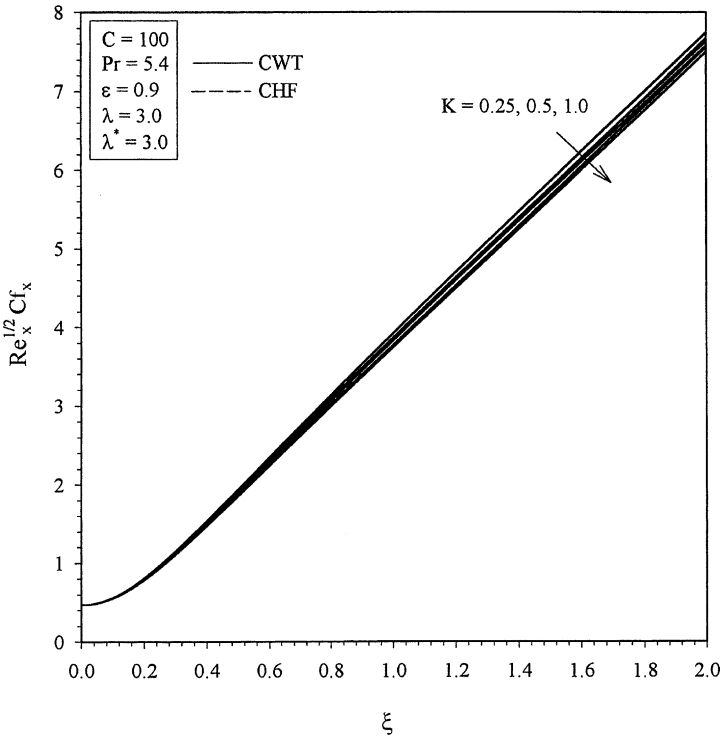

Fig. 10. Effect of K on $Re_x^{1/2}Cf_x$ for CWT and CHF cases.

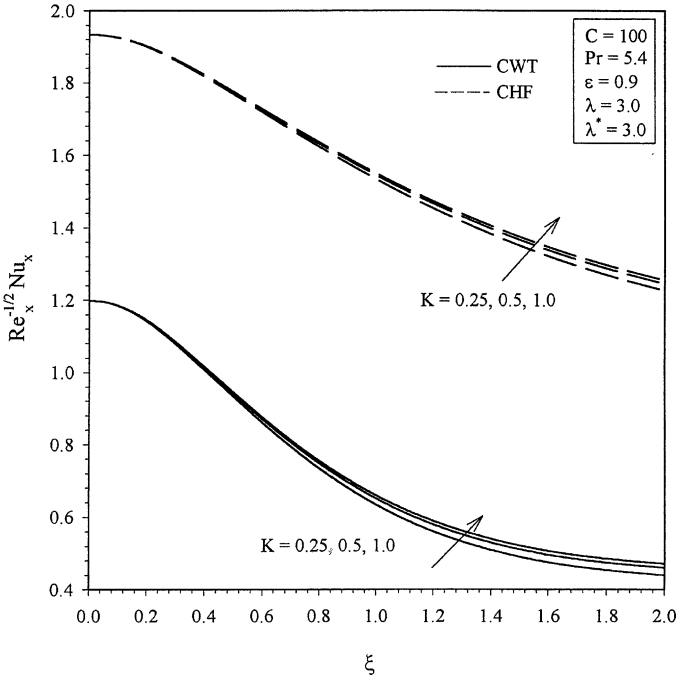

Fig. 11. Effect of K on $Re_x^{-1/2} Nu_x$ for CWT and CHF cases.

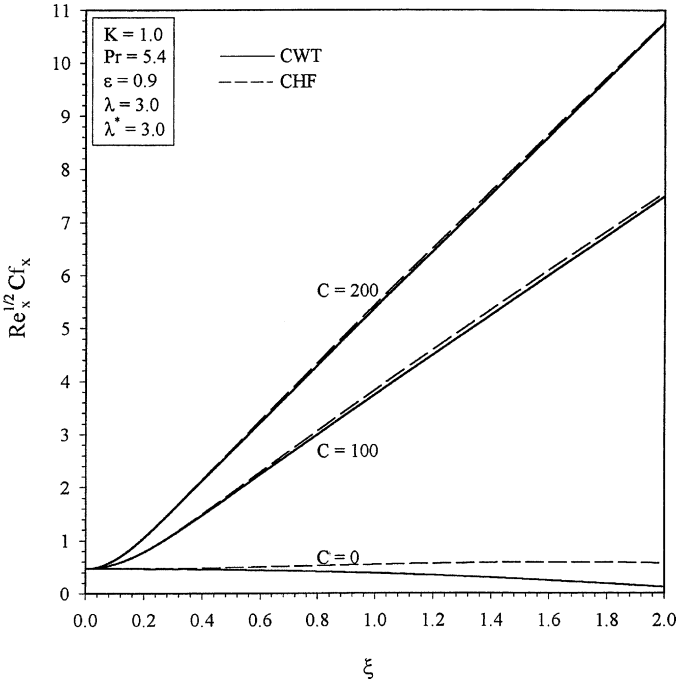

Fig. 12. Effect of C on $Re_x^{1/2} Cf_x$ for CWT and CHF cases.

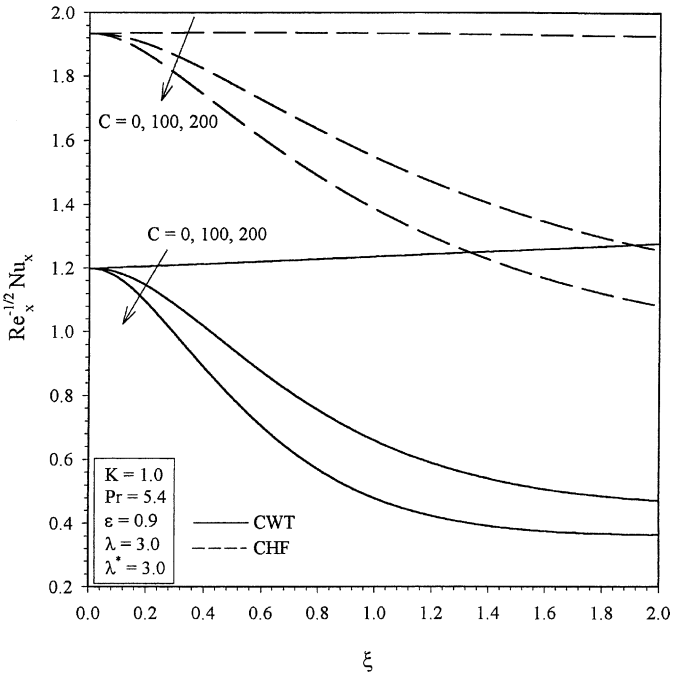

Fig. 13. Effect of C on $Re_x^{-1/2}Nu_x$ for CWT and CHF cases.

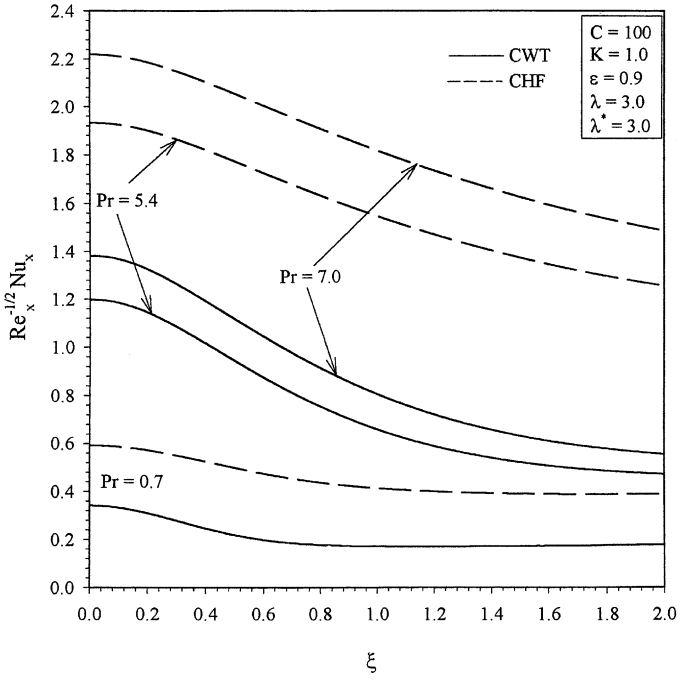

Fig. 14. Effect of Pr on $Re_x^{-1/2}Nu_x$ for CWT and CHF cases.

5. Conclusions

The Nusselt number and the skin friction are significantly affected by the inertia and porosity parameters, whereas the effect of the permeability parameter on them is rather small. The Prandtl number and the buoyancy force influence significantly the Nusselt number, but the skin friction coefficient is very little affected. The Nusselt number for the constant heat flux case is significantly more than that of the constant wall temperature case, whereas there is very little difference in the skin fractions for the constant wall temperature and constant heat flux cases.

References

[1] M.A. Combarnous, S.A. Bories, Hydro-thermal convection in saturated porous media, Adv. Hydrosci. 10 (1975) 231–307.
[2] A. Bejan, The method of scale analysis: natural convection in porous media, in: W. Aung, S. Kakac, S. Viskanta (Eds.), Natural Convection: Fundamentals and Applications, Hemisphere, Washington, DC, 1985, pp. 548–572.
[3] A. Bejan, Convective heat transfer in porous media, in: S. Kakac, R.K. Shah, W. Aung (Eds.), Handbook of Single-Phase Convective Heat Transfer, Wiley, New York, 1987, Chapter 6.
[4] C.L. Tien, K. Vafai, Convective and radiative heat transfer in porous media, Adv. Appl. Mech. 27 (1989) 225–281.
[5] C.K. Chen, C.I. Hung, H.C. Horng, Transient natural convection on a vertical flat plate embedded in a high-porosity medium, ASME J. Energy Res. Tech. 109 (1987) 112–118.
[6] C.K. Chen, C.R. Lin, Natural convection from an isothermal vertical surface embedded in a thermally stratified high-porosity medium, Int. J. Eng. Sci. 33 (1995) 131–138.
[7] A.J. Chamkha, Hydromagnetic natural convection from an isothermal inclined surface adjacent to a thermally stratified porous medium, Int. Eng. Sci. 35 (1997) 975–986.
[8] B.J. Minto, D.B. Ingham, I. Pop, Free convection driven by an exothermic reaction on a vertical surface embedded in porous media, Int. J. Heat Mass Transfer 41 (1998) 11–24.
[9] D.A.S. Rees, I. Pop, Vertical free convection in a porous medium with variable permeability effect, Int. J. Eng. Sci. 38 (2000) 2565–2572.
[10] E.J. Le Fevre, A.J. Ede, Laminar free convection from the outer surface of a vertical circular cylinder, Proc. Appl. Mech. 4 (1956) 175–183.
[11] H.R. Hama, J.V. Recesso, J. Christiaens, The axisymmetric free convection temperature field along a vertical thin cylinder, J. Aerospace 26 (1959) 335–342.
[12] W.J. Minkowycz, E.M. Sparrow, Local non-similarity solutions for natural convection on a vertical cylinder, J. Heat Transfer 96 (1974) 178–183.
[13] T. Cebeci, Laminar free convection heat transfer from the outer surface of a vertical slender circular cylinder, in: Proceedings of the International Heat Transfer Conference N.C., vol. 1.4, 1974, pp. 15–19.
[14] E.M. Sparrow, J.L. Gregg, Laminar free convection heat transfer from the outer surface of a vertical circular cylinder, J. Heat Transfer 78 (1956) 1823–1829.
[15] H.K. Kuiken, Axisymmetric free convection boundary layer flow past lender bodies, Int. J. Heat Mass Transfer 11 (1968) 1141–1153.
[16] T. Fuji, H. Uchara, Laminar natural convective heat transfer from the outer surface of a vertical cylinder, Int. J. Heat Mass Transfer 13 (1970) 607–615.
[17] A. Aziz, T.Y. Na, Improved perturbation solutions for laminar natural convection on a vertical cylinder, Thermo-Fluid Dyn. 16 (1982) 83–87.
[18] A. Pantokratarás, Laminar natural convection of pure and saline water along a vertical isothermal cylinder, Heat Mass Transfer 36 (2000) 351–360.
[19] B.C. Sakiadis, Boundary layer behaviour on continuous surface III. The boundary layer on a continuous surface, A.I.Ch.E.J. 7 (1961) 467–470.

[20] D.E. Bourne, D.G. Elliston, Heat transfer through the axially symmetric boundary layer on a moving circular fibre, Int. J. Heat Mass Transfer 13 (1970) 583–593.
[21] J. Karnis, V. Pechoc, The thermal laminar boundary layer on a continuous cylinder, Int. J. Heat Mass Transfer 21 (1978) 43–47.
[22] I.G. Choi, The effect of variable properties of air on the boundary layer for a moving continuous cylinder, Int. J. Heat Mass Transfer 25 (1982) 597–602.
[23] T.Y. Na, I. Pop, Flow and heat transfer over a longitudinal circular cylinder moving in a parallel or reversely to a free stream, Acta Mech. 118 (1996) 185–195.
[24] F.G. Blottner, Finite-difference methods of solution of the boundary layer equations, AIAA J. 8 (1970) 193–205.
[25] P.K. Tsou, E.M. Sparrow, K.J. Goldstein, Flow and heat transfer in the boundary layer on a continuous moving surface, Int. J. Heat Mass Transfer 10 (1967) 219–235.
[26] L.E. Erickson, L.T. Fan, V.G. Fox, Heat and mass transfer on a moving continuous flat plate with suction or blowing, Ind. Eng. Chem. Fund. 5 (1966) 19–25.
[27] J.F. Griffin, J.L. Thorne, On the thermal boundary layer growth on continuous moving belts, A.I.Ch.E.J. 13 (1967) 1210–1214.
[28] A. Moutsoglou, T.S. Chen, Buoyancy effects in boundary layers on inclined continuous moving sheets, J. Heat Transfer 102 (1980) 171–173.